JOURNAL OF AGRICULTURAL AND FOOD CHEMISTRY

Stability of Ferric Complexes with 3-Hydroxyflavone (Flavonol), 5,7-Dihydroxyflavone (Chrysin), and 3′,4′-Dihydroxyflavone

MARK D. ENGELMANN,‡ RYAN HUTCHESON, AND I. FRANCIS CHENG*

Department of Chemistry, University of Idaho, Moscow, Idaho 83844-2343

The acid dissociation and ferric stability constants for complexation by the flavonoids 3-hydroxyflavone (flavonol), 5,7-dihydroxyflavone (chrysin), and 3′,4′-dihydroxyflavone in 50:50 (v/v) ethanol/water are determined by pH potentiometric and spectrophotometric titrations and the linear least-squares curve-fitting program Hyperquad. Over the entire range of pH and reagent concentrations spanning the titration experiments, the stoichiometry for iron−flavonoid complex formation was 1:1 for all three flavonoids examined. The three flavonoids were chosen for their hydroxy substitution pattern, with each possessing one of the three most commonly suggested sites for metal binding by the flavonoids. On the basis of the calculated stability constants, the intraflavonoid-binding site competition is illustrated as a function of pH via speciation curves. The curves indicate that the binding site comprised of the 3′,4′-hydroxy substitutions, the catecholic site, is most influential for ferric complexation at the physiological pH of 7.4. The possibility for antioxidant activity by flavonoid chelation of ferric iron in the presence of other competitive physiological complexing agents is demonstrated through additional speciation calculations.

INTRODUCTION

It has been well-established that flavonoids, the largest group of polyphenolic phytochemicals, are effective scavengers of radicals *in vitro* (*1*−*3*) and thereby capable of an antioxidant effect (*4*). In theory, a radical scavenger should be present in excess relative to both the radical and the components that it is meant to protect to be effective. On the other hand, antioxidants that prevent the formation of the oxyradicals should be capable of an effect at much lower concentrations. Such prevention may result from the chelation of pro-oxidant first-row transition metals.

There is a growing body of evidence that suggests certain flavonoids may be able to exert an antioxidant effect as metal chelates of iron in particular (*5*−*10*). Such effects would result from the moderation of the iron−oxygen chemistry responsible for the formation of oxyradicals. For example, the Fenton reaction (eq 1) involves the generation of hydroxyl radicals from hydrogen peroxide by an iron complex.

$$Fe^{II}L + H_2O_2 \rightarrow Fe^{III}L + HO^- + HO\cdot \qquad (1)$$

The specific ligand, L, in eq 1 influences both the thermodynamics and kinetics of the reaction. The standard reduction potential, $E°$, of the FeL complex depends heavily upon the electron-donation properties of the ligand. Oxydonors, for example, tend to decrease the standard reduction potential, which in turn tends to stabilize the ferric, trivalent state. If flavonoids, as oxychelates, are acting as antioxidants by iron chelation, they would favor the ferric state. Thus, the stability constants for flavonoid−ferric complexation must be favored over ferric complexes with other physiologically relevant ligands. In this manner, flavonoids may be capable of displacing pro-oxidant ligands from ferric iron to form complexes of high stability, thereby preventing its redox cycling and further oxidative damage. A precise measure of the ferric−flavonoid stability constants is therefore crucial.

The polyphenolics commonly referred to as flavonoids include several structural classes, but they all share the same common flavan base structure, pictured in **Figure 1**. Substitution about the C ring defines each class of flavonoid, and substitution about the A and B rings distinguish individual members of each class. For example, keto substitution at the 4 position in conjunction with dehydrogenation at carbons 2 and 3 define the flavone class. This class of flavonoids is most often associated with metal chelation and thus will be the focus of this study.

Within the flavone class, hydroxy substitution at the 3 position defines a subclass of flavone, the flavonols. A common flavonol is quercetin, pictured in **Figure 1**. Quercetin is often cited as one of the more potent antioxidant of the flavonoid series (*11*−*18*). A previous electrochemical study established that quercetin was able to prevent the Fe^{II}−ATP complex from undergoing the Fenton reaction in a 1:1 molar ratio (*12*). Quercetin is a pentahydroxy-flavone with three potential sites for the chelation of cations. These are the catechol moiety on the B ring, between the 4-keto and 3-hydroxy groups of the C ring, and between the 4-keto and 5-hydroxy groups of the C and A rings. The

* To whom correspondence should be addressed: Department of Chemistry, University of Idaho, Moscow, ID 83844-2343. Telephone: 208-885-6387. E-mail: ifcheng@uidaho.edu.

‡ Present address: Pacific Northwest National Laboratory, P. O. Box 999 MSIN P8-50, Richland, WA 99352.

10.1021/jf048298q CCC: $30.25
Published on Web 03/26/2005

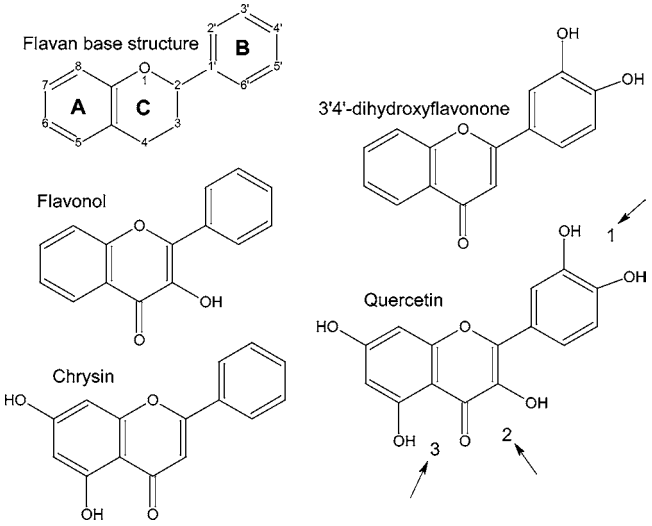

Figure 1. Flavonoids used for this study. Also, the flavan base structure with the conventional ring labeling and numbering patterns indicated. Quercetin is also pictured with the three commonly cited metal-binding sites highlighted.

potential for competitive binding at all three sites makes stability constant determination for any given site difficult, and should the binding isotherms for sites severely overlap, site-specific stability constant calculations will be nearly impossible. Nonetheless, such measurements have been attempted on quercetin, yet still, the precise site of binding is not known (*19*, *20*).

To elucidate the logical binding site on the quercetin ring system for Fe^{III}, the stability constants for complex formation between the three model flavones (one for each potential binding site, pictured in **Figure 1**) 3-hydroxyflavone (flavonol), 5,7-dihyroxyflavone (chrysin), and 3′,4′-dihydroxy-flavone (3′,4′-DHF) and iron are measured in a water/ethanol-mixed solvent medium. These constants are then used to suggest the preferred binding site as a function of pH and examine the potential speciation of the three flavonols given a simulated physiological medium.

EXPERIMENTAL PROCEDURES

Materials. Quercetin dihydrate (99%), chrysin (99%+), and 1,2-dihydroxybenzene-3,5-disulfonic acid, disodium salt (tiron) were purchased from Acros, NJ; flavonol was purchased from Aldrich, WI; and 3′,4′-DHF (97%) was purchased from Lancaster, NH. Standard solutions of NaOH and HNO_3 were prepared from concentrated solutions and standardized with potassium hydrogen phthalate (KHP). Ferric nitrate heptahydrate was purchased from Fisher, NJ. Water was doubly distilled, boiled to remove CO_2 and carbonate, and then stored with Ascarite CO_2 traps. Ethanol (200 proof) was purchased from AAPER of KY and sparged with dry nitrogen prior to use to remove dissolved CO_2.

Instrumentation/Apparatus. UV−visible spectra were recorded on a Hewlett−Packard (now Agilent) 8453 diode array. An error function relating the standard deviation in the measurement as a function of absorbance was developed for this instrument according to the procedure outlined in Hyperquad (*21*). Potentiometry involved the use of a Denver Instruments combination pH electrode, and a Model 15 Accumet pH meter was calibrated according to the method of Gran and adapted for the given solvent (*22*−*24*). Hyperquad has a built-in error function for potentiometry that assumes that the error in the voltage reading is proportional to the slope of the titration curve for the given data point. The titration cell consisted of a double-walled glass beaker connected to a Fisher Isotemp water bath maintained at 25.0 ± 0.1 °C and fitted with a sealable Teflon cap drilled to allow a continuous N_2 purge and sample access. The N_2 purge gas was saturated with the appropriate solvent so as to maintain a constant solvent volume and composition. The titrant was added using a Denver Instruments Titrator 280 manual titrator.

General Methods. The cell was loaded with 15.00 mL of flavonoid solution, which was premixed in a volumetric flask. The solvent composition was 44.6-weight percent ethanol in water (24.0 mole percent), which is achieved by adding half the volume of a volumetric flask with water and diluting to the mark with ethanol. The autoprotolysis constant for the given solvent system has been determined previously to be $10^{-14.4}$ (*21*); this value was used for all subsequent stability constant calculations. The titrations were performed using the described cell apparatus and titrator with in situ pH measurement and flavonoid concentration of approximately 0.50 mM for the potentiometry. The ionic strength was maintained at 0.050 M with $NaNO_3$, and the titrant was 0.050 M NaOH standardized regularly with primary standard potassium hydrogen phthalate and phenolphthalein indicator. For reasons described in the Results and Discussion, only the chrysin proton constants were determined by potentiometry; all other complexation equilibria were more adequately monitored by spectrophotometric methods.

Spectrophotometric measurements were obtained through periodic sampling of the titration solution, which contained the flavonoids at concentrations of 25 μM. After absorbance measurement, the solution was returned to the titration cell and the process was repeated until titration completion. Proton equilibria were determined using standardized 2.0 mM NaOH as the titrant.

The metal complexation titrations involved two methods: with flavonol, competition between the proton and ferric ions for the 3-hydroxy/4-keto-binding site provided the measure of ferric−flavonol complex stabiltiy. To the 25 μM solution of flavonol, enough standardized HNO_3 was added to achieve a concentration of 0.10 M H^+. To this, a solution of 2.0 mM ferric nitrate was added as the titrant, which displaced the proton and formed the characteristic red/purple ferric−flavonol complex. Chrysin and 3′,4′-DHF do not bind ferric iron under the acidic conditions required to prevent the formation of solid ferric hydroxides. Therefore, 1,3-disulfato-4,5-dihydroxybenzene (tiron) was used as a competing ligand and delivered as 10 mM titrant to a solution of the preformed ferric−chrysin and ferric−3′,4′-DHF complexes. The solutions are unbuffered and slightly acidic to begin with because of the protons displaced by complexation to the ferric ion from the acid form of the flavonoids. The tiron is added as the basic sodium salt; therefore, the solution eventually becomes buffered at basic pH because of the presence of excess tiron. In this way, a range of pH that extends well below and above physiological pH is covered. The use of competing ligands for the determination of β for complexes of high stability has become widely practiced (*25*, *26*). It becomes necessary with large stability constant (β) values because of the inherent difficulty in measuring the concentrations for the free ligand and metal for an equilibrium that is shifted so far to the products (complex). To use the tiron as a competing ligand, its ferric ion equilibria had to be determined for the given solvent composition. The conditions for these measurements were duplicated from the literature (*27*) with the exception of the solvent.

Data Analysis. Data were analyzed by importing absorbance values into the Hyperquad2000 stability constant calculation software program. A detailed description of the Hyperquad suite of programs and algorithms used is presented in the literature (*28*), but in general, the program calculates stability constants from potentiometric and spectrophotometric titration data by a linear least-squares curve-fitting analysis. The stability constants are reported as β_{MLH}, where M, L, and H designate metal, ligand, and hydrogen, respectively.

RESULTS AND DISCUSSION

Titrations. Flavonol and all flavonoid−ferric complexes are insoluble above about 50 μM. Below this concentration, pH potentiometric measurements are difficult. Furthermore, the second ionization of 3′,4′-DHF occurs at very high pH, which both damages the glass pH electrode and strongly interferes with the pH measurement because of the high sodium ion concentra-

Table 1. Flavonoid–Proton and Flavonoid–Ferric Equilibrium Constants[a]

chrysin	pK_a/logβ	rmsd	σ	χ^2
proton 1	7.90	0.010	1.07	27.1
proton 2	11.40	0.011	1.07	27.1
ferric iron	11.40	0.028	2.45	7.52
flavonol				
proton	9.99	0.016	3.84	4.44
ferric iron	13.29	0.021	3.22	7.45
3′,4′-dihydroxyflavone				
proton 1	8.39	0.079	4.63	5.80
proton 2	13.43	0.038	4.80	11.6
ferric iron	20.87	0.039	3.27	13.24

[a] Proton constants are expressed as the conventional negative logarithm of the stepwise acid dissociation constants, pK_a, and the flavonoid–ferric constants are expressed as the logarithm of the overall stability constant, logβ.

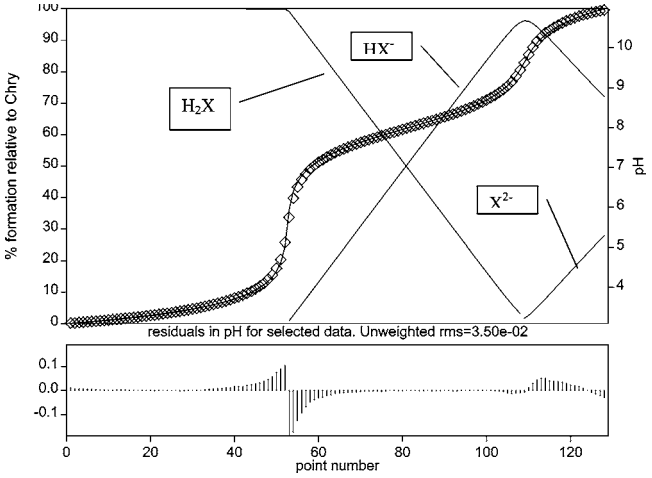

Figure 2. Potentiometric pH titration curve for chrysin. Diamonds are experimental data points. The line through the points is the modeled curve, and the histogram below is the unweighted residuals in units of pH between experimental and model points. Speciation of the three forms of chrysin, H_2chrysin (H_2X), [H-chrysin]$^-$ (HX^-), and [chrysin]$^{2-}$ (X^{2-}), are given as a function of the titration point.

tion. For these reasons, spectrophotometry was favored for equilibrium measurements except for the determination of the chrysin (solubility > 50 μM) protonation constants.

Explanation of Statistics Used in the Hyperquad Program. The potentiometry-determined values of β_{011} and β_{012} (β_{MLH}) for the flavonoid−proton complexes and for the Fe^{III}−flavonoid complexes and β_{110} are given in **Table 1** along with their standard deviations, which are calculated on the basis of the statistical set of all data points (β is calculated at each point in the titration). χ^2 is the sum of the weighted residuals and is used primarily as a tool for interpreting the effects of certain variables on the refined value of β. The σ value for the chrysin refinement of 1.07 is very nearly a perfect result. σ is the primary measure of the goodness-of-fit for the model that serves as the basis for β. In the case of spectrophotometric titrations analyzed through Hyperquad, the additional tools of the factor analyses and molar absorbances calculated from the refined β parameter are also crucial for the assessment of β. The validity of β cannot be unequivocally proven by any one of the previously mentioned criteria. It must be assessed in consideration of all available data, and that therein is the advantage that Hyperquad holds over traditional methods of stability constant calculation. The stability constant, β, may be calculated for a given equilibrium by traditional means, which rely very heavily on simplifying assumptions, the validity of which are quite often suspect and lacking in a systematic form of proof. Additionally, β is quite often obtained from such calculations on a single data point; thus, the value is entirely without a statistical measure of model error.

Chrysin Protontation Constants. The proton complexes of chrysin were examined successfully by pH potentiometry. The solubility of chrysin is substantially higher than that of flavonol because of the additional hydroxy substitution, and its second proton ionization occurs within the upper pH limit requirement of the glass pH electrode. The pH potentiometric titration curve of chrysin is shown in **Figure 2**. From **Figure 2**, it can be seen that, during the pH potentiometric titration, the second proton dissociation only occurred to roughly 25% rather than the ideal 50% at the final pH of 11 (the limit of the glass-bulb pH electrode). Attempts to track the second proton dissociation spectrophotometrically failed because of a lack of significant differences between the spectra of [H-chrysin]$^-$ and [chrysin]$^{2-}$, thus, the use of the potentiometric result. On the other hand, the potentiometric refinement was quite successful. Using the model consisted of the following:

$$H_2\text{chyrsin} = H - \text{chrysin}^- + H^+ \qquad K_{a1} \qquad (2)$$

$$H - \text{chrysin}^- = \text{chrysin}^{2-} + H^+ \qquad K_{a2} \qquad (3)$$

Optimized Hyperquad fitted the model titration curve in **Figure 2** (continuous curve) to the experimental data (◇) based on a least-squares analysis of K_{a1} and K_{a2}. The points of highest residual difference, apparent on the residual histogram in **Figure 2** (bottom), were at the inflection points where the error in pH is greatest with respect to the volume of titrant added. Otherwise, the model fit is a very good match for the experimental titration curve. The pK_a values for the two ionizable protons were found to be 7.90 and 11.40 for chrysin (**Table 1**).

Flavonol Protontation Constants. Flavonol presents a very clear example of the spectrophotometric titration process. **Figure 3** displays a series of spectra illustrating a classic spectrophotometric titration with two very distinct isosbestic points. The protonated form of flavonol gives a maximum at 346 nm, which decreases as the NaOH titrant is added, giving rise to the deprotonated form with a maximum at 410 nm. **Figure 3B** illustrates the decrease in absorbance at 346 nm as NaOH titrant is added. **Figure 3C** represents the deconvoluted spectra for H-flavonol and (flavonol)$^-$ as analyzed by Hyerquad at point 24 of the titration curve (**Figure 3B**). There is no evidence of any other species in solution. The existence of other equilibrium species may be eliminated through the use of the factor analyses tools included in the Hyperquad software. The mathematics of factor analysis is beyond the scope of this manuscript, and the reader is once again referred to Gans et al. (*21*, *28*). However, the chemical implication is that the eigenvector analysis provides a statistical test and visual display for the number of light-absorbing species involved in the equilibrium over the range of titration points and wavelengths studied. The eigenvector display produces a smooth curve for every correctly deduced light-absorbing species; each additional incorrectly hypothesized species results in a "failed" eigenvector plot (**Figure 3E**), which is manifested as a noisy curve. The basis for the eigenvector analysis is that the absorbance at any given wavelength is the sum of absorbances for all light-absorbing species present in the equilibrium. Thus, all of the spectroscopic information necessary for the solutions to the mass-balance equations is contained in the spectrum. However, it must be deconvoluted

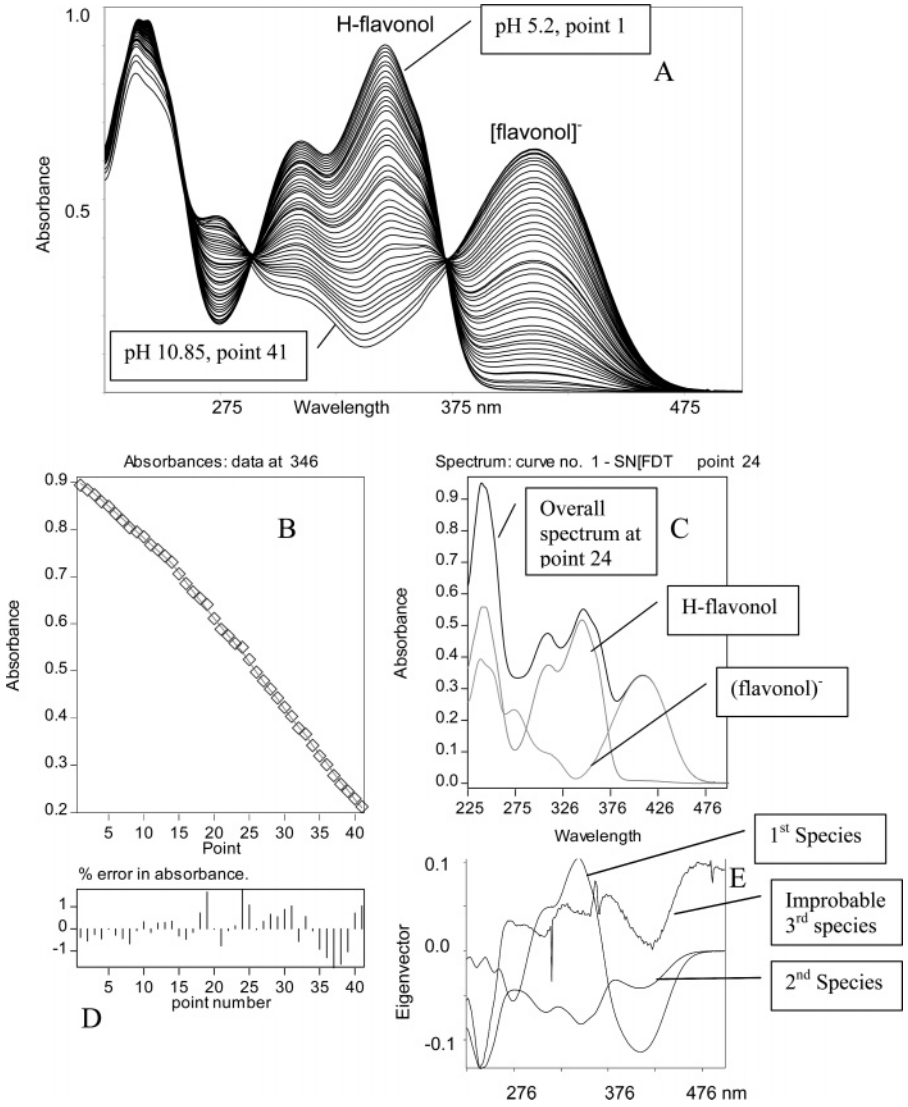

Figure 3. (A) Spectrophotometric titration spectra for flavonol. The titration begins with the spectrum of maximum absorbance at 346 nm, H-flavonol, at pH 5.2, titration point 1, and finishes with the spectrum of maximum absorbance at 410 nm, $(flavonol)^-$, at pH 10.85, titration point 41. (B) Postrefinement spectrophotometric titration curve at 346 nm of the pH titration of flavonol. The titration begins with H-flavonol and ends with $(flavonol)^-$. The line is fitted to the individual data points (◇) by Hyperquad. (C) Individual (lower two curves) and overall (uppermost) spectra for the pH titration of H-flavonol system at point 24 of the spectrophotometric titration (curve B). The deconvoluted individual contributions to the overall spectrum were obtained by Hyperquad. The deconvoluted spectra are in good agreement with the spectra of the individual species shown in curve A. See also the eigenvector analysis in curve E. (D) Unweighted residuals at each point of the titration in curve B in units of error in percent absorbance. (E) Eigenvector analysis for the H-flavonol/$(flavonol)^-$ system at point 24 in B. The analysis demonstrates that a 3rd species is highly unlikely.

to provide the absorptivities. Deconvolution is possible if a collection of spectra are obtained sequentially, such as in a titration or during elution from a column. The eigenvectors are the matrix solutions for postulated equilibrium species; solutions exist for correctly deduced species, whereas only noise exists for superfluous attempts.

Sometimes the result of the eigenvector plot is somewhat ambiguous. Hyperquad utilizes a second factor analysis, the singular value decomposition, which provides an additional test for the same result, the number of light-absorbing species in solution. The process is similar; only the result is a series of positive singular values at each titration point for correctly deduced absorbing species. Incorrectly attempted factors result in singular values of zero, and the curve for such a factor is generally lost in the *x* axis with a series of values very near to zero. The difference between the two factor analyses is that one is displayed as a function of the wavelength, while the other is a function of the titration point. Therefore, one result may be clear when the other is somewhat ambiguous. For example, a species may contribute to the overall spectrum for only a small portion of the optical window under investigation, or a species may appear toward the end of the titration. A comparison of the two factor analyses becomes particularly important as the complexity of the equilibrium system increases and the number of light-absorbing entities grows. For the systems described in this work, the two factor analyses were always in agreement. The fitted Hyperquad analysis (**Figure 3B**) for the spectrophotometric pH titration of flavonol indicated a pK_a of 9.99 for the lone ionizable proton. The wavelengths used for the statistical analysis were 309, 346, and 410 nm.

3′4′-DHF Protontation Constants. The acid dissociation constants for 3′4′-DHF were also measured by spectrophotometric pH titration. The Hyperquad analysis of 3′,4′-DHF generates distinct spectra for all three forms of the flavonoid, i.e., H_2-3′,4′-DHF, H-3′,4′-DHF, and 3′,4′-DHF^{2-}. The determination of the first proton dissociation constant was routine;

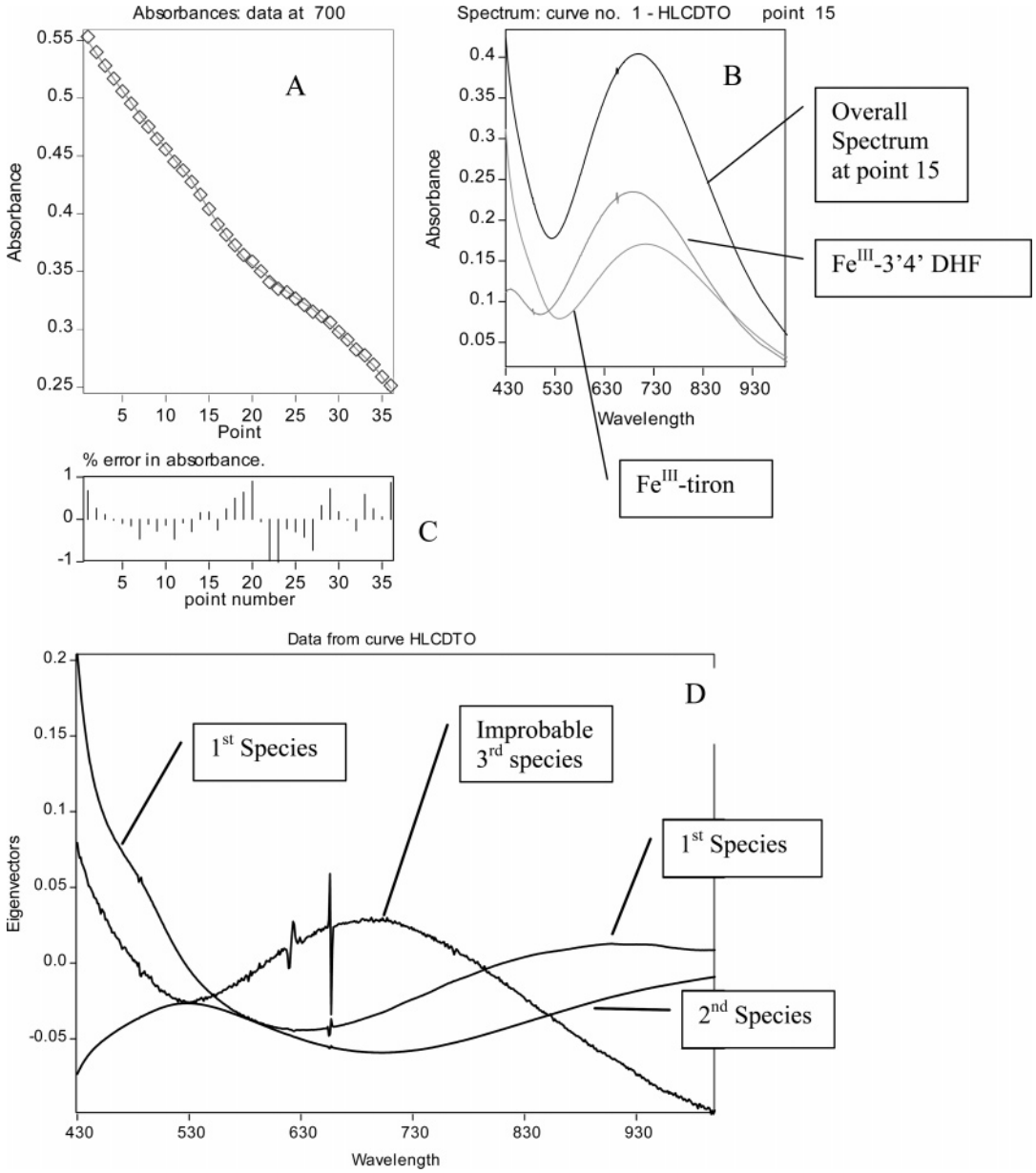

Figure 4. (A) Postrefinement spectrophotometric titration curve at 700 nm of the 3′,4′-dihydroxyflavone–ferric complex with tiron. The titration begins with the lone ferric–flavonoid complex at point 1 and proceeds with the displacement of the flavonoid by tiron to form the Fe^{III}–tiron complex. The line is fitted to the individual data points (◇) by Hyperquad. (B) Individual (lower two curves) and overall (uppermost) spectra for the ferric/3′,4′-DHF/tiron system at point 15 of the spectrophotometric titration (A). The maximum at 700 nm corresponds to the ferric–3′,4′-DHF complex. As tiron is added, the 3′,4′-DHF is displaced and the maximum is shifted to a slightly longer wavelength corresponding to the ferric–tiron complex (lowest curve). The deconvoluted individual contributions to the overall spectrum were obtained by Hyperquad. (C) Unweighted residuals at each point of the titration in curve A in units of error in percent absorbance. (D) Eigenvector analysis for the Fe^{III}/3′,4′-DHF/tiron system at point 15 in A. The analysis demonstrates that a 3rd species is highly unlikely.

however, the determination of β_{012} was somewhat difficult. An imperfect fit is evident in the patterned residuals, and also in the large σ value in **Table 1**. It is likely that the highly alkaline conditions (pH 13.5) required for the ionization of the second catecholic proton resulted in the hydrolysis or polymerization of the flavonol; both effects have been reported (*29*, *30*) and observed as a part of this work on the flavonoid quercetin. However, the effect is likely minimal, and the refined parameter of log β_{012} of 13.43 is both an acceptable fit and chemically reasonable value for a second catecholic proton, which are of known high stability. All pK_a values for each of the three examined flavonoids are summarized in **Table 1**. The wavelengths used in the Hyperquad analysis for the two ionizable protons were 233, 344, and 405 nm and 272, 303, 334, 406, and 450 nm, respectively.

Fe^{III}−3′,4′-DHF Stability Constant. Spectrophotometry was again utilized for the determination of β_{110} for the three studied Fe^{III}−flavonoid complexes. The spectral characteristics and data analyses for one titration point (number 15) in **Figure 4A** are shown in **Figure 4B**, which shows the distinctly different molar absorbances of the two species contributing to the overall spectra for the visible range studied. The uppermost curve in **Figure 4B** is the overall spectrum of the Fe^{III}−3′,4′-DHF where tiron is added as a titrant. The two bottom curves in **Figure 4B** are the deconvoluted curves for individual spectra of Fe^{III}−3′,4′-DHF and Fe^{III}−tiron, respectively. The eigenvetor analysis

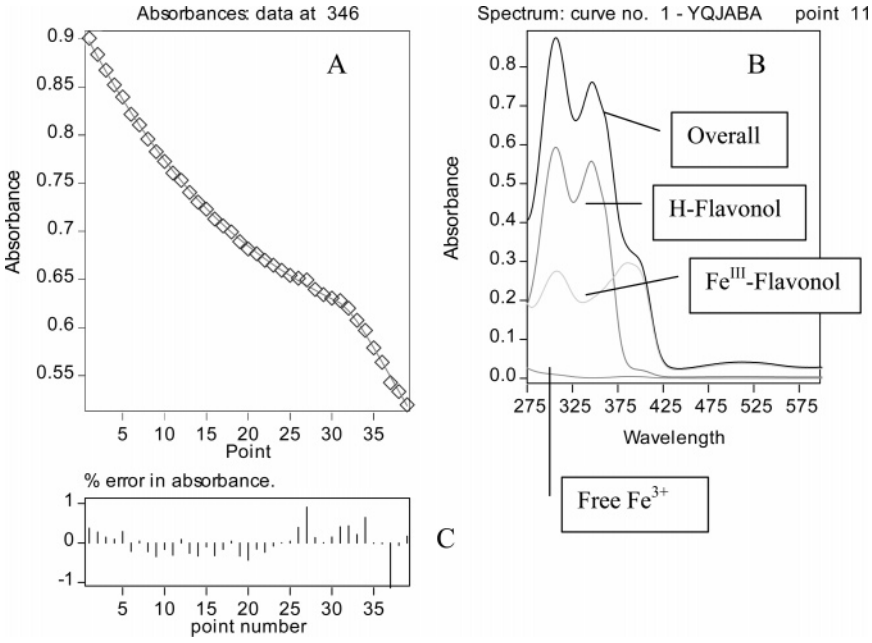

Figure 5. (A) Postrefinement spectrophotometric titration curve at 346 nm of flavonol with ferric iron. The titration begins with the lone flavonol at point 1 and proceeds to nearly complete complexation by point 40 as the ferric iron is added as a titrant. The line is fitted to the individual data points (◇) by Hyperquad. (B) Individual (lower curves) and overall (uppermost) spectra for the ferric flavonol system at point 11 of the spectrophotometric titration. The maximum at 346 nm corresponds to the protonated flavonol in 0.10 M nitric acid. As the ferric ions are added, the proton is displaced and the maximum is shifted to longer wavelength corresponding to the ferric–flavonol complex. The weak contribution comes from the excess ferric ions, which are yellow in the mixed aqueous/ethanol solvent. (C) Unweighted residuals at each point of the titration (A) in units of error in percent absorbance.

(**Figure 4D**) for the titration curve reveals that only two species are present, i.e., Fe^{III}−3′,4′-DHF and Fe^{III}−tiron. Thus, the model for the titration curve is based on the displacement reaction

$$Fe^{III}-3',4'\text{-DHF} + \text{tiron} = Fe^{III}-\text{tiron} + 3',4'\text{-DHF} \quad (4)$$

Only the 1:1 metal/ligand stoichiometries were observed. This is consistent with the bulk of the literature available on the subject. A least-squares analyses by Hyperquad that takes into account each titration point at seven different wavelengths (680, 690, 700, 710, 720, 730, and 740 nm) indicates that the log β_{110} for the Fe^{III}−3′,4′-DHF complex is 20.87 (**Table 1**).

Fe^{III}−Chrysin Stability Constant. In the case of Fe^{III}−chrysin [the 1:1 Fe^{III}−chrysin complex is more correctly described by a β of the following form: β_{111}, where the third "1" indicates that the complex still retains the proton at the 7 position (at least at pH < 6). However, it is more intuitive to compare the value for β_{110}, as if the proton is not involved in the complexation of the iron, which, in this case, it does not. Therefore, in this manner, $\log\beta_{110} = 11.40$, whereas $\log\beta_{111} = 19.30(\log\beta_{110} + \log\beta_{012} - \log\beta_{011})$], the result of the factor analyses are unambiguous; only two light-absorbing species exist: Fe^{III}−tiron (1:1 stoichiometry only) and Fe^{III}−chrysin. This is not to suggest that no other species are involved in the equilibrium, quite the contrary. An excess of tiron was necessary to affect significant binding of the ferric ion; therefore, an excess of free tiron was always present. However, free tiron is invisible at the studied wavelengths (660, 665, 670, and 675 nm). The statistical analyses outlined in **Figure 4** yielded a stability constant (β_{110}) of 11.40 (**Table 1**).

Fe^{III}−Flavonol Stability Constant. The pH titration of flavonol was measured by UV−visible absorbance spectrophotometry (**Figure 5**). The spectral shifts that occur as a result of the complexation of iron and flavonol are evident in **Figure 5B**, the UV−visible spectra of flavonol in the absence and presence of excess ferric ion as deconvoluted from the overall spectrum. The 346 nm transition was used for the calculation of β_{110}. The titration for this equilibrium system involved the addition of $Fe(NO_3)_3$ as a titrant in the presence of an initial 0.10 M HNO_3. At this pH, an excess of ferric ion is required to fully bind the flavonol; thus, there will be some free ferric ions in solution by the end of titration. In ethanol, ferric salts are quite soluble and yellow in solution. Therefore, the free iron will make some contribution to the observed spectrum. This is confirmed in the eigenvector analysis, where three smooth functions are evident (free Fe^{3+}, H-flavonol, and Fe^{III}−flavonol) and the fourth is subject to noise. The statistics for the determination of β_{110} for ferric−flavonol, presented in **Table 1**, when combined with the additional measures of assessment for β, suggest an adequate model. The stability constants for the Fe^{III}−flavonol complex were refined using absorptivities at 307, 346, and 389 nm.

Significance of Study and Likelihood of Physiological Iron Binding. Using the acid dissociation and stability constants summarized in **Table 1**, it is possible to generate speciation plots to estimate the predominant species at physiological pH given a solution of iron with molar equivalents of each of the three model flavonols. Such a plot, as calculated by HySS (Hyperquad Speciation and Simulation), along with literature values for ferric−hydroxo complexes, is presented in **Figure 6** (*31*). A similar plot, pictured in **Figure 7**, may be constructed for a combination of the studied flavonols present with various ligands of physiological importance. The ligands chosen along with their concentrations were taken from a study of the speciation in blood plasma (*32*). While localized cellular concentrations may deviate from this, it illustrates the utility of the calculated flavonoid stability constants. Ligand stability constants were obtained from the NIST database (*33*).

From the speciation diagrams, it can be concluded that, of the tested flavonols, the 3′,4′-DHF will have the greatest iron-

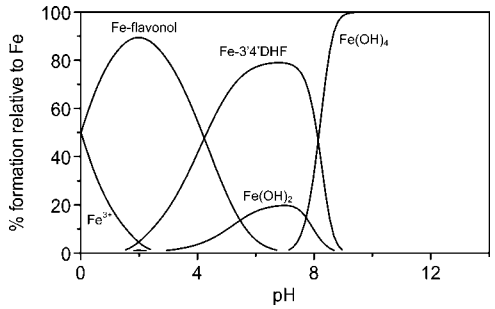

Figure 6. Speciation of 1.0 mM each of Fe^{3+}, flavonol, chrysin, and 3′,4′-dihydroxyflavone. Chrysin is included in the calculation, but the stability constant for complex formation with Fe^{III} is low enough that it constitutes less than 1% of the mass balance of iron and therefore does not appear on the speciation diagram.

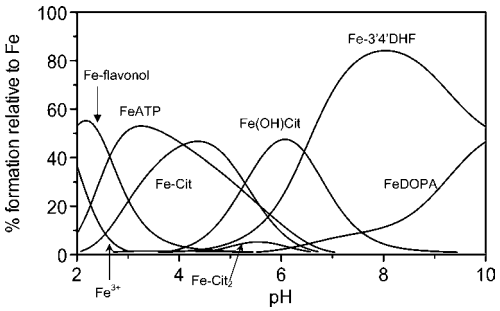

Figure 7. Speciation of the following: 1 μM Fe^{3+}, 5 μM each of the three studied flavonols, 1 μM DOPA, 11 μM citrate, 48 μM glutamate, 37 μM alanine, and 10 μM ATP. Chrysin complexes with Fe^{III} are of low enough stability that they account for less than 1% of the mass balance of iron. $Fe(OH)_n$, soluble ferric–hydroxo complexes, are omitted for clarity.

binding capacity at physiological pH and that the 5-hydroxy position is likely not important for binding with iron. It is also likely that there is a region of overlap from about pH 2−6 where a flavonoid possessing both the catechol-binding site on the B ring and the 3-hydroxy-binding site on the A ring will likely be capable of forming complexes of the stoichiometry M_2L. This fact should be taken into account in studies of flavonoids with both sites present.

Figure 7 indicates that, in the presence of a variety of physiologically relevant ligands, the examined flavonols do present competition in the form of low-molecular-weight complexes with ferric ion. Again, it is the 3′,4′-DHF with the catecholic binding site that figures most prominently at physiological pH. Only DOPA, itself a catecholic metal chelate, binds significantly at higher pH than 3′,4′-DHF. The logβ for Fe^{III}−DOPA is 21.9 and is actually greater than that measured for Fe^{III}−3′,4′-DHF (20.9) but so are the stabilities for the proton equilibria (pK_{a1} = 13.4 and pK_{a2} = 23.2 for DOPA, and pK_{a1} = 13.4 and pK_{a2} = 21.8 for 3′,4′-DHF). Thus, at the critical pH value of 7.4, the Fe^{III}−3′,4′-DHF constitutes about 80% of the iron mass balance.

Importance of the Catecholic Site in Flavonoid Structure−Activity Relationships. From this, it can be concluded that flavonoids in possession of the catecholic binding site, i.e., 3′,4′-hydroxyl groups on the B ring, are capable of antioxidant activity through Fe^{III} chelation, at least from the standpoint that such flavonoids are capable of pro-oxidant ligand displacement. Indeed, it appears that the catechol moiety in the B ring figures prominently in the antioxidant structure−activity relationships of flavonoids (*34*−*39*).

ACKNOWLEDGMENT

The authors thank Peter Gans for his assistance with the Hyperquad Software package.

LITERATURE CITED

(1) Lin, Y.; Wu, S.; Lin, J. Determination of tea polyphenols and caffeine in tea flowers (*Camellia sinensis*) and their hydroxyl radical scavenging and nitric oxide supressing effects. *J. Agric. Food Chem.* **2003**, *51*, 975−980.

(2) Lien, E. J.; Ren, S.; Bui, H.; Wang, R. Quantitative structure activity relationship analysis of phenolic antioxidants. *Free Radical Biol. Med.* **1999**, *26*, 285−294.

(3) Hanasaki, Y.; Shunjiro, O.; Fukui, S. The correlation between active oxygens scavenging and antioxidant effects of flavonoids. *Free Radical Biol. Med.* **1994**, *16*, 845−850.

(4) Bors, W.; Heller, W.; Michel, C.; Saran, M. Flavonoids as antioxidants: Determination of radical scavenging efficiencies. *Methods Enzymol.* **1990**, *186*, 343−355.

(5) Ferrali, M.; Signorini, B.; Caciotti, B.; Sugherini, L.; Ciccoli, L.; Giachetti, D.; Comporti, M. Protection against oxidative damage of erythrocyte membrane by the flavonoid quercetin and its relation to iron chelating activity. *FEBS Lett.* **1997**, *416*, 123−129.

(6) Kuo, S.; Leavitt, P. S.; Lin, C. Dietary flavonoids interact with trace metals and affect metallothionein level in human intestinal cells. *Biol. Trace Elem. Res.* **1998**, *62*, 135−153.

(7) Morel, I.; Lescoat, G.; Cillard, P.; Cillard J. Role of flavonoids and iron chelation in antioxidant action. *Methods Enzymol.* **1994**, *234*, 437−443.

(8) Romanova, D.; Valchalkova, A.; Cipak, L.; Ovesna, Z.; Rauko, P. Study of antioxidant effect of apigenin luteolin and quercetin by DNA protective method. *Neoplasma* **2001**, *48*, 104−107.

(9) Yoshino, M.; Murakami, K. Interaction of iron with polyphenolic compounds: Application to antioxidant characterization. *Anal. Biochem.* **1998**, *257*, 40−44.

(10) Sestilli, P.; Diamantini, G.; Bedini, A.; Cerioni, L.; Tommasini, I.; Tarzia, G.; Cantoni, O. Plant derived phenolic compounds prevent the DNA single strand breakage and cytotoxicity induced by *tert*-butylhydroperoxide via an iron chelating mechanism. *Biochem. J.* **2002**, *364*, 121−128.

(11) Sugita, O.; Ishizawa, N.; Matsuto, T.; Okada, M.; Kayahara, N. A new method of measuring the antioxidant activity of polyphenols using cumene hydroperoxide. *Ann. Clin. Biochem.* **2004**, *41*, 72−77

(12) Cheng, I. F.; Breen, K. On the ability of four flavonoids, baicilein, luteolin, naringenin, and quercetin, to suppress the fenton reaction of the iron−ATP complex. *Biometals* **2000**, *13*, 77−83.

(13) Benninger, C. W.; Hosfield, G. L. Antioxidant activity of extracts, condensed tannin fractions, and pure flavonoids from *Phaseolus vulgaris* L. seed coat color genotypes. *J. Agric. Food Chem.* **2003**, *51*, 7879−7883.

(14) Guzy, J.; Kunir, J.; Marekova, M.; Chakova, Z.; Dubayova, K.; Mojiova, G.; Mirossay, L. Effect of quercetin on daunorubicin-induced heart mitochondria changes in rats. *Physiol. Res.* **2003**, *52*, 773−780.

(15) Chun, O. K.; Kim D.-O.; Moon, H. Y.; Kang, H. G.; Lee, C. Y. Contribution of individual polyphenolics to total antioxidant capacity of plums, *J. Agric. Food Chem.* **2003**, *51*, 7240−7245.

(16) Peng I.-W.; Kuo, S.-M. Flavonoid structure affects the inhibition of lipid peroxidation in caco-2 intestinal cells at physiological concentrations. *J. Nutr.* **2003**, *133*, 2184−2187.

(17) Hendricks, J. A.; de Vries, H. E.; van der Pol, S. M..A.; van den Berg, T. K.; van Tol, E. A. F.; Dijkstra, C. D. Flavonoids inhibit myelin phagocytosis by macrophages; a structure−activity relationship study. *Biochem. Pharmacol.* **2003**, *65*, 877−885.

(18) Matsuda, H.; Morikawa, T.; Toguchida, I.; Yoshikawa, M. Structural requirements of flavonoids and related compounds for aldose reductase inhibitory activity. *Chem. Pharm. Bull.* **2002**, *50*, 788−795.

(19) Escandar, G. M.; Sala, L. F. Complexing behavior of rutin and quercetin. *Can. J. Chem.* **1991**, *69*, 1994−2001.
(20) Cotelle, N. Role of flavonoids in oxidative stress. *Curr. Top. Med. Chem.* **2001**, *1*, 569−590.
(21) HYPERQUAD, software programs was acquired from Prof. Peter Gans, Department of Inorganic and Structural Chemistry, University of Leeds, Leeds, U.K.
(22) Gran, G. Determination of the equivalence point in potentiometric titrations. Part II. *Analyst* **1952**, *77*, 661.
(23) Johansson, A.; Gran, G. Automatic titration by stepwise addition of equal volumes of titrant. Part V. Extension of the Gran I method for calculation of the equivalence volume in acid−base titrations. *Analyst* **1980**, *105*, 802−810.
(24) Inoue, M.; Fernando, Q. Effect of dissolved CO_2 on Gran plots. *J. Chem. Educ.* **2001**, *78*, 1132−1135.
(25) Clark, N. H.; Martell, A. E. Ferrous chelates of EDTA, HEDTA, and SHBED. *Inorg. Chem.* **1988**, *27*, 1297−1298.
(26) Stolworthy, J. C. R. Stability of flavonoid complexes of copper-(II) and flavonoid antioxidant activity. *Anal. Chim. Acta* **1976**, *85*, 375−381.
(27) Chatlas, J.; Jordan, R. B. Complexation of the aqua−iron(III) dimer by tiron: Kinetics of complex formation and dissociation. *Inorg. Chem.* **1994**, *33*, 3817−3822.
(28) Gans, P.; Vacca, A.; Sabatini, A. Investigation of equilibria in soluiton: Determination of equilibrium constants with the hyperquad suite of programs. *Talanta* **1996**, *43*, 1739−1753.
(29) Thompson, M.; Williams, C. R.. Stability of flavonoid complexes of copper(II) and flavonoid antioxidant activity. *Anal. Chim. Acta* **1976**, *85*, 375−381.
(30) Mellican, R. I.; Li, J.; Mehansho, H.; Nielsen, S. S. The role of iron and the factors affecting off-color development of polyphenols. *J. Agric. Food Chem.* **2003**, *51*, 2304−2316.
(31) Smith R. M.; Martell A. E. Critical stability constants. Plenum Press: New York 1975; Vols. 1−4.
(32) Konigsberger, L.; Konigsberger, E.; May, P. M.; Hefter, G. T. Complexation of iron(III) by citrate. Implications for iron speciation in blood plasma. *J. Inorg. Biochem.* **2000**, *78*, 97−103.
(33) Motekaitis, R. J.; Smith, R. M.; Martell, A. E. NIST critically selected stability constants of metal complexes database, version 5.0; NIST Standard Reference Database 46, http://www.nist.gov/srd/webguide/nist46/46_5.htm.
(34) Heim, K. E.; Tagliaferro, A. R.; Bobilya, D. J. Flavonoid antioxidants: Chemistry, metabolism, and structure−activity relationships. *J. Nutr. Biochem.* **2002**, *13*, 572−584.
(35) van Acker, S. A.; van den Berg, D. J.; Tromp, M. N.; Griffioen, D. H.; van Bennekom , W. P.; van der Vijgh, W. J.; Bast, A. Structural aspects of antioxidant activity of flavonoids. *Free Radical Biol. Med.* **1996**, *20*, 331−342.
(36) Kumamoto, M.; Sonda, T.; Nagayama, K.; Tabata, M. Effects of pH and metal ions on antioxidative activities of catechins. *Biosci. Biotechnol. Biochem.* **2001**, *65*, 126−132.
(37) Heijnen, C. G.; Haenen, G. R.; Oostveen, R. M.; Stalpers, E. M.; Bast, A. Protection of flavonoids against lipid peroxidation: The structure activity relationship revisited. *Free Radical Res.* **2002**, *36*, 575−581.
(38) Mira, L.; Fernandez, M. T.; Santos, M.; Rocha, R.; Florencio, M. H.; Jennings, K. R. Interactions of flavonoids with iron and copper ions: A mechanism for their antioxidant activity. *Free Radical Res.* **2002**, *36*, 1199−1208.
(39) Silva, M. M.; Santos, M. R.; Caroco, G.; Rocha, R.; Justino, G.; Mira, L. Structure−antioxidant activity relationships of flavonoids: A re-examination. *Free Radical Res.* **2002**, *36*, 1219−1227.

Received for review October 13, 2004. Revised manuscript received March 3, 2005. Accepted March 7, 2005. This work was funded by an NIH Grant 1 R15 GM062777-01.

JF048298Q